



**HAL**  
open science

## A Visibility Information for Multi-Robot Localization

Rémy Guyonneau, Sébastien Lagrange, Laurent Hardouin

► **To cite this version:**

Rémy Guyonneau, Sébastien Lagrange, Laurent Hardouin. A Visibility Information for Multi-Robot Localization. IEEE/RJS International Conference on Intelligent Robots and Systems (IROS), Nov 2013, Tokyo, Japan. hal-00874164

**HAL Id: hal-00874164**

**<https://hal.science/hal-00874164>**

Submitted on 19 Jan 2021

**HAL** is a multi-disciplinary open access archive for the deposit and dissemination of scientific research documents, whether they are published or not. The documents may come from teaching and research institutions in France or abroad, or from public or private research centers.

L'archive ouverte pluridisciplinaire **HAL**, est destinée au dépôt et à la diffusion de documents scientifiques de niveau recherche, publiés ou non, émanant des établissements d'enseignement et de recherche français ou étrangers, des laboratoires publics ou privés.

# A Visibility Information for Multi-Robot Localization

Rémy Guyonneau, Sébastien Lagrange and Laurent Hardouin

**Abstract**—This paper proposes a set-membership method based on interval analysis to solve the pose tracking problem for a team of robots. The originality of this approach is to consider only weak sensor data: the visibility between two robots. The paper demonstrates that with this poor information, without using bearing or range sensors, a localization is possible. By using this boolean information (two robots see each other or not), the objective is to compensate the odometry errors and be able to localize in an indoor environment all the robots of the team, in a guaranteed way. The environment is supposed to be defined by two sets, an inner and an outer characterizations. This paper mainly presents the visibility theory used to develop the method. Simulated results allow to evaluate the efficiency and the limits of the proposed algorithm.

## I. INTRODUCTION

Robot localization is an important issue in mobile robotics [1], [2], [3] since it is one of the most basic requirement for many autonomous tasks. The objective is to estimate the pose (position and orientation) of a mobile robot by using the knowledge of an environment (*e.g.* a map) and sensor data.

In this paper the pose tracking problem is considered: the objective is to compute the current pose of a robot knowing its previous one and avoiding its drifting. To compensate the drifting, due to odometry errors, external data are necessary. Contrary to most of the localisation approaches that use range sensors [4], [5], [6] this paper tends to prove that only *weak* informations can lead to an efficient localization too. The information to be considered is the visibility between robots: two robots are visible if there is no obstacle between them, else there are not visible. It can be noticed that visibility sensors have already been considered for localization and mapping [7], [8], [9]. But those approaches associate the visibility information to bearing and/or range measurements. In this paper the proposed visibility corresponds to a boolean information (true or false), illustrated in Figure 1 and presented in Section III. This information can be obtained using 360° camera for example.

Note that the presented visibility information does not depend of the robots' orientations (it is assumed that the robots can *see* all around themselves). In order to simplify the localization problem it is assumed that each robots are equipped with a compass. Thus the objective is to estimate the position  $\mathbf{x}_i = (x_{1_i}, x_{2_i})$  of a robot  $r_i$ .

A robot  $r_i$  is characterized by the following discrete time dynamic equation:  $\mathbf{q}_i(k+1) = f(\mathbf{q}_i(k), \mathbf{u}_i(k))$ , with  $k$  the discrete time,  $\mathbf{q}_i(k) = (\mathbf{x}_i(k), \theta_i(k))$  the pose of the robot,  $\mathbf{x}_i(k) = (x_{1_i}(k), x_{2_i}(k))$  its position,  $\theta_i(k)$  its orientation (associated to the compass) and  $\mathbf{u}_i(k)$  the input vector (associated to the odometry). The function  $f$  characterizes the robot's

dynamics. In order to exploit the visibility information a team of  $n$  robots  $\mathcal{R} = \{r_1, \dots, r_i, \dots, r_n\}$  is considered.

The environment is assumed to be an indoor environment  $\mathcal{E}$  composed by  $m$  obstacles  $\varepsilon_j$ ,  $j = 1, \dots, m$ . This environment is not known perfectly but is characterized by two known sets:  $\mathcal{E}^-$  an inner characterization, and  $\mathcal{E}^+$  an outer characterization, presented in the Section II-B.

To solve this problem a set-membership approach of the localization problem based on interval analysis is considered as in [10], [11].

## II. ALGEBRAIC TOOLS

This section introduces some algebraic useful tools.

### A. Interval analysis

An *interval vector* [12], or a *box*  $[\mathbf{x}]$  is defined as a closed subset of  $\mathbb{R}^n$ :  $[\mathbf{x}] = ([x_1], [x_2], \dots) = ([x_1, \bar{x}_1], [x_2, \bar{x}_2], \dots)$ .

The size of an *interval*  $[x_1]$  is defined as  $w([x_1]) = (\bar{x}_1 - x_1)$ . For instance  $w([2, 5]) = 3$ .

It can be noticed that any arithmetic operators such as  $+$ ,  $-$ ,  $\times$ ,  $\div$  and functions such as *exp*, *sin*, *sqr*, *sqrt*, ... can be easily extended to intervals, [13].

A Constraint Satisfaction Problem (CSP) is defined by three sets. A set of variables  $V$ , a set of domains  $D$  for those variables and a set of constraints  $C$  connecting the variables together. Example of CSP:

$$\left\{ \begin{array}{l} V = \{x_1, x_2, x_3\} \\ D = \{x_1 \in [7, +\infty], x_2 \in [-\infty, 2], x_3 \in [-\infty, 9]\} \\ C = \{x_1 = x_2 + x_3\} \end{array} \right\}. \quad (1)$$

Solving a CSP consists into reducing the domains by removing the values that are not consistent with the constraints. It can be efficiently solved by considering interval arithmetic [14]. For the example (1):

$$\begin{aligned} x_1 = x_2 + x_3 &\Rightarrow x_1 \in [x_1] \cap ([-\infty, 2] + [-\infty, 9]), \\ &\Rightarrow x_1 \in [7, +\infty] \cap [-\infty, 11] = [7, 11]. \\ x_2 = x_1 - x_3 &\Rightarrow x_2 \in [x_2] \cap ([7, 11] - [-\infty, 9]), \\ &\Rightarrow x_2 \in [-\infty, 2] \cap [-2, +\infty] = [-2, 2]. \\ x_3 = x_1 - x_2 &\Rightarrow x_3 \in [x_3] \cap ([7, 11] - [-2, 2]), \\ &\Rightarrow x_3 \in [-\infty, 2] \cap [5, 13] = [5, 13]. \end{aligned}$$

The solutions of that CSP are the following contracted domains  $[x_1]^* = [7, 11]$ ,  $[x_2]^* = [-2, 2]$  and  $[x_3]^* = [5, 13]$ . In this example a *backward/forward* propagation method is used to contract the domains. The *forward* propagation refers to the contraction of  $[x_1]$ , then the earned information is propagated to the domains  $[x_2]$  and  $[x_3]$ , which corresponds to the *backward* step. In the proposed localization method, the backward/forward propagation is used to contract the robots' poses.

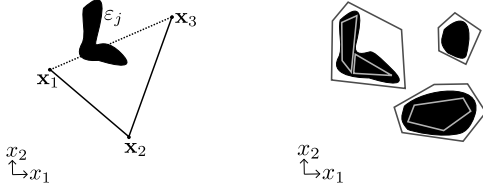


Fig. 1. In the **left figure**:  $(\mathbf{x}_1 \mathbf{V} \mathbf{x}_2)_{\varepsilon_j}$ ,  $(\mathbf{x}_2 \mathbf{V} \mathbf{x}_3)_{\varepsilon_j}$  and  $(\mathbf{x}_1 \bar{\mathbf{V}} \mathbf{x}_3)_{\varepsilon_j}$ . The **right figure** illustrates an environment  $\mathcal{E}$  (black shapes) and its characterizations  $\mathcal{E}^-$  (light grey segments) and  $\mathcal{E}^+$  (dark grey segments). It can be noticed that an obstacle can have an empty inner characterization.

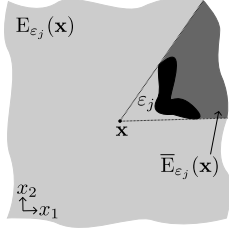


Fig. 2. The light grey space represents  $E_{\varepsilon_j}(\mathbf{x})$  whereas the dark grey space represents  $\bar{E}_{\varepsilon_j}(\mathbf{x})$ . The black shape corresponds to  $\varepsilon_j$ .

### B. The environment and its characterizations

An environment  $\mathcal{E} = \bigcup_{j=1}^m \varepsilon_j$  corresponds to a set of  $m$  obstacles, with  $\varepsilon_1, \dots, \varepsilon_j, \dots, \varepsilon_m$  connected subsets of  $\mathbb{R}^2$ .

The environment is never known perfectly but always approximated, using maps for example. In order to deal with uncertain environments and to provide guaranteed results, we consider an inner  $\mathcal{E}^-$  and an outer  $\mathcal{E}^+$  characterizations of the environment  $\mathcal{E}$  such that  $\mathcal{E}^- \subseteq \mathcal{E} \subseteq \mathcal{E}^+$ .

Those characterizations are considered to be sets of segments (Figure 1):  $\mathcal{E}^- = \bigcup_{j=1}^{m'} \varepsilon_j^{s-}$  and  $\mathcal{E}^+ = \bigcup_{j=1}^{m''} \varepsilon_j^{s+}$ , with  $\varepsilon_j^s = \text{Seg}(\mathbf{e}_{1j}, \mathbf{e}_{2j})$  the segment defined by the points  $\mathbf{e}_{1j}$  and  $\mathbf{e}_{2j}$ .

## III. VISIBILITY PRESENTATION

All the points and sets are assumed to be in  $\mathbb{R}^2$ .

### A. Point Visibility

1) *According to an obstacle  $\varepsilon_j$* : The visibility relation between two points  $\mathbf{x}_1, \mathbf{x}_2$  regards to an obstacle  $\varepsilon_j$  is defined as  $(\mathbf{x}_1 \mathbf{V} \mathbf{x}_2)_{\varepsilon_j} \Leftrightarrow \text{Seg}(\mathbf{x}_1, \mathbf{x}_2) \cap \varepsilon_j = \emptyset$ , with  $\text{Seg}(\mathbf{x}_1, \mathbf{x}_2)$  the segment defined by the two points  $\mathbf{x}_1$  and  $\mathbf{x}_2$ .

The complement of this relation, named the non-visibility relation, is denoted  $(\mathbf{x}_1 \bar{\mathbf{V}} \mathbf{x}_2)_{\varepsilon_j}$ .

Examples of visibility and non-visibility relations are presented Figure 1. It can be noticed that

$$(\mathbf{x}_1 \bar{\mathbf{V}} \mathbf{x}_3)_{\varepsilon_j} \Leftrightarrow \text{Seg}(\mathbf{x}_1, \mathbf{x}_3) \cap \varepsilon_j \neq \emptyset, \quad (2)$$

$$(\mathbf{x}_1 \mathbf{V} \mathbf{x}_2)_{\varepsilon_j} \Leftrightarrow (\mathbf{x}_2 \mathbf{V} \mathbf{x}_1)_{\varepsilon_j}, \text{ (Symmetric)} \quad (3)$$

$$(\mathbf{x}_1 \bar{\mathbf{V}} \mathbf{x}_3)_{\varepsilon_j} \Leftrightarrow (\mathbf{x}_3 \bar{\mathbf{V}} \mathbf{x}_1)_{\varepsilon_j}. \quad (4)$$

The visible space of a point  $\mathbf{x}$  regards to an obstacle  $\varepsilon_j$  with  $\mathbf{x} \cap \varepsilon_j = \emptyset$ , is defined as  $E_{\varepsilon_j}(\mathbf{x}) = \{\mathbf{x}_i | (\mathbf{x} \mathbf{V} \mathbf{x}_i)_{\varepsilon_j}\}$ , and the non-visible space of  $\mathbf{x}$  regards to  $\varepsilon_j$  is defined as  $\bar{E}_{\varepsilon_j}(\mathbf{x}) = E_{\varepsilon_j}^c(\mathbf{x})$ .

Examples of visible and non-visible spaces are presented in Figure 2.

2) *According to an environment  $\mathcal{E}$* : As the robots are moving in a environment  $\mathcal{E}$  composed by  $m$  obstacles, it is needed to extend the previous definitions to multiple obstacles:

$$(\mathbf{x}_1 \mathbf{V} \mathbf{x}_2)_{\mathcal{E}} \Leftrightarrow \text{Seg}(\mathbf{x}_1, \mathbf{x}_2) \cap \mathcal{E} = \emptyset, \quad (5)$$

$$E_{\mathcal{E}}(\mathbf{x}) = \{\mathbf{x}_i | (\mathbf{x} \mathbf{V} \mathbf{x}_i)_{\mathcal{E}}\}, \quad (6)$$

$$E_{\mathcal{E}}^c(\mathbf{x}) = \bar{E}_{\mathcal{E}}(\mathbf{x}). \quad (7)$$

It is possible to characterize the visibility over an environment by considering the visibility regards to the obstacles that composed this environment.

*Lemma 1*: Let  $\mathbf{x}_1$  and  $\mathbf{x}_2$  be two distinct points and  $\mathcal{E}$  an environment, with  $\mathbf{x}_1 \notin \mathcal{E}$  and  $\mathbf{x}_2 \notin \mathcal{E}$ . Then

$$(\mathbf{x}_1 \mathbf{V} \mathbf{x}_2)_{\mathcal{E}} \Leftrightarrow \bigwedge_{j=1}^m (\mathbf{x}_1 \mathbf{V} \mathbf{x}_2)_{\varepsilon_j}, \quad (8)$$

$$(\mathbf{x}_1 \bar{\mathbf{V}} \mathbf{x}_2)_{\mathcal{E}} \Leftrightarrow \bigvee_{j=1}^m (\mathbf{x}_1 \bar{\mathbf{V}} \mathbf{x}_2)_{\varepsilon_j}. \quad (9)$$

*Lemma 2*: Let  $\mathbf{x}$  be a point and  $\mathcal{E}$  an environment such as  $\mathbf{x} \notin \mathcal{E}$ . Then

$$E_{\mathcal{E}}(\mathbf{x}) = \bigcap_{j=1}^m E_{\varepsilon_j}(\mathbf{x}), \quad (10)$$

$$\bar{E}_{\mathcal{E}}(\mathbf{x}) = \bigcup_{j=1}^m \bar{E}_{\varepsilon_j}(\mathbf{x}). \quad (11)$$

3) *According to the environment characterizations  $\mathcal{E}^+$  and  $\mathcal{E}^-$* : As noticed in the Section II-B, the environment is not known but characterized by two sets,  $\mathcal{E}^+$  and  $\mathcal{E}^-$ . The following lemma provides a relation between the visibility according to the environment and the characterizations.

*Lemma 3*: Let  $\mathbf{x}_1$  and  $\mathbf{x}_2$  be two points,  $\mathcal{E}$  an environment such as  $\mathbf{x} \notin \mathcal{E}$ , and  $\mathcal{E}^-$  and  $\mathcal{E}^+$  the inner and outer characterizations of the environment. Then

$$(\mathbf{x}_1 \mathbf{V} \mathbf{x}_2)_{\mathcal{E}} \Rightarrow (\mathbf{x}_1 \mathbf{V} \mathbf{x}_2)_{\mathcal{E}^-}, \quad (12)$$

$$(\mathbf{x}_1 \bar{\mathbf{V}} \mathbf{x}_2)_{\mathcal{E}} \Rightarrow (\mathbf{x}_1 \bar{\mathbf{V}} \mathbf{x}_2)_{\mathcal{E}^+}. \quad (13)$$

### B. Set Visibility

This Section extends the visibility notions to connected sets. Let  $\mathbb{X}$  be a connected set and  $\varepsilon_j$  an obstacle such as  $\mathbb{X} \cap \varepsilon_j = \emptyset$ . The visible space of  $\mathbb{X}$  regards to  $\varepsilon_j$  is defined as  $E_{\varepsilon_j}(\mathbb{X}) = \{\mathbf{x}_i | \forall \mathbf{x} \in \mathbb{X}, (\mathbf{x} \mathbf{V} \mathbf{x}_i)_{\varepsilon_j}\}$ .

The non-visible space of  $\mathbb{X}$  regards to  $\varepsilon_j$  is defined as  $\bar{E}_{\varepsilon_j}(\mathbb{X}) = \{\mathbf{x}_i | \forall \mathbf{x} \in \mathbb{X}, (\mathbf{x} \bar{\mathbf{V}} \mathbf{x}_i)_{\varepsilon_j}\}$ .

*Remark 1*: When considering a set, a third visibility space has to be defined. This space, named partial-visibility space, corresponds to all the points that are neither in the visible nor non-visible spaces of the set:

$$\tilde{E}_{\varepsilon_j}(\mathbb{X}) = \{\mathbf{x}_i | \exists \mathbf{x}_1 \in \mathbb{X}, \exists \mathbf{x}_2 \in \mathbb{X}, (\mathbf{x}_1 \mathbf{V} \mathbf{x}_i)_{\varepsilon_j} \wedge (\mathbf{x}_i \bar{\mathbf{V}} \mathbf{x}_2)_{\varepsilon_j}\}. \quad (14)$$

Examples of visibility spaces considering a connected set are presented in the Figure 3.

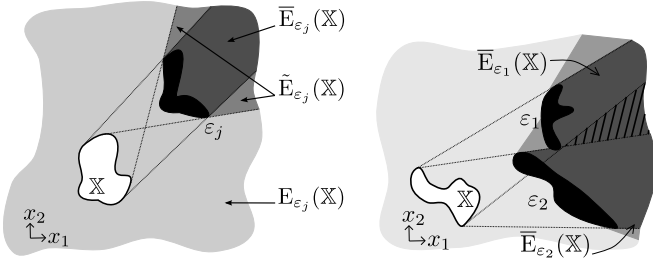


Fig. 3. **Left Figure:** The light grey space represents  $E_{\epsilon_j}(\mathbb{X})$ , the dark grey space represents  $\bar{E}_{\epsilon_j}(\mathbb{X})$  and the medium grey space represents  $\tilde{E}_{\epsilon_j}(\mathbb{X})$ . The black shape corresponds to  $\epsilon_j$  and the white one to  $\mathbb{X}$ . **Right Figure:** In this example it can be noticed that  $\bar{E}_{\epsilon}(\mathbb{X})$  (the union of the hatched and dark grey) includes  $\bar{E}_{\epsilon_1}(\mathbb{X}) \cup \bar{E}_{\epsilon_2}(\mathbb{X})$  (dark grey without hatched).

It is possible to extend those notions to an environment

$$E_{\mathcal{E}}(\mathbb{X}) = \{\mathbf{x}_i | \forall \mathbf{x} \in \mathbb{X}, (\mathbf{x} \vee \mathbf{x}_i)_{\mathcal{E}}\}, \quad (15)$$

$$\bar{E}_{\mathcal{E}}(\mathbb{X}) = \{\mathbf{x}_i | \forall \mathbf{x} \in \mathbb{X}, (\mathbf{x} \bar{\vee} \mathbf{x}_i)_{\mathcal{E}}\}. \quad (16)$$

The visibility over an environment can be characterized by considering the visibility regards to the obstacles that composed this environment.

*Lemma 4:* Let  $\mathbb{X}$  be a connected and  $\mathcal{E}$  an environment with  $\mathbb{X} \cap \mathcal{E} = \emptyset$ . Then,

$$E_{\mathcal{E}}(\mathbb{X}) = \bigcap_{j=1}^m E_{\epsilon_j}(\mathbb{X}), \quad (17)$$

$$\bar{E}_{\mathcal{E}}(\mathbb{X}) \supseteq \bigcup_{j=1}^m \bar{E}_{\epsilon_j}(\mathbb{X}). \quad (18)$$

Figure 5 illustrates the inclusion of Equation 18.

The following lemma provides a relation between the visibility according to the environment and the characterizations. This represents the basis of the proposed localization method.

*Lemma 5:* Let  $\mathbf{x}_1 \in \mathbb{X}_1$  and  $\mathbf{x}_2 \in \mathbb{X}_2$  be two distinct points, with  $\mathbb{X}_1, \mathbb{X}_2$  two connected sets such as  $\mathbb{X}_1 \cap \mathbb{X}_2 = \emptyset$ . Considering an environment  $\mathcal{E}$  with its characterizations  $\mathcal{E}^+$  and  $\mathcal{E}^-$

$$(\mathbf{x}_1 \vee \mathbf{x}_2)_{\mathcal{E}} \Rightarrow \begin{cases} \mathbb{X}_1 \subseteq \mathbb{X}_1 \cap (\bigcap_{j=1}^{m'} \bar{E}_{\epsilon_j^c}(\mathbb{X}_2)) \\ \mathbb{X}_2 \subseteq \mathbb{X}_2 \cap (\bigcap_{j=1}^{m'} \bar{E}_{\epsilon_j^c}(\mathbb{X}_1)) \end{cases} \quad (19)$$

$$(\mathbf{x}_1 \bar{\vee} \mathbf{x}_2)_{\mathcal{E}} \Rightarrow \begin{cases} \mathbb{X}_1 \subseteq \mathbb{X}_1 \cap (\bigcup_{j=1}^{m''} E_{\epsilon_j^c}(\mathbb{X}_2)) \\ \mathbb{X}_2 \subseteq \mathbb{X}_2 \cap (\bigcup_{j=1}^{m''} E_{\epsilon_j^c}(\mathbb{X}_1)) \end{cases} \quad (20)$$

This lemma is an extension of Lemma 3.

#### IV. THE CONTRACTORS

In this section the two contractors  $C_V([\mathbf{x}_1], [\mathbf{x}_2], \epsilon_j^s)$  and  $C_{\bar{V}}([\mathbf{x}_1], [\mathbf{x}_2], \epsilon_j^s)$  are presented. A contractor is an operator that can remove the points of the domains ( $[\mathbf{x}_1]$  and  $[\mathbf{x}_2]$ ) that are not consistent with a given constraint (visibility information). In our case the contractor  $C_V$  contracts over the visibility relation and  $C_{\bar{V}}$  over the non-visibility relation. The Figure 5 presents an example of contraction according to the visibility and non-visibility. Those contractors are based on Equations 19 and 20. It can be noticed that the computation of the visible and non-visible spaces  $E_{\epsilon_j^s+}([\mathbf{x}_2])$

and  $\bar{E}_{\epsilon_j^s-}([\mathbf{x}_2])$  are needed to contract the domains  $[\mathbf{x}_1]$  and  $[\mathbf{x}_2]$ .

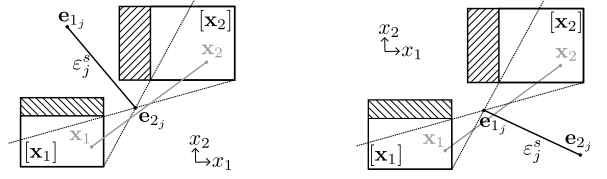


Fig. 4. **Left Figure:** Let  $\mathbf{x}_1 \in [\mathbf{x}_1]$  and  $\mathbf{x}_2 \in [\mathbf{x}_2]$  be two points such that  $(\mathbf{x}_1 \vee \mathbf{x}_2)_{\epsilon_j^s}$ , then using the contractor  $C_V([\mathbf{x}_1], [\mathbf{x}_2], \epsilon_j^s)$  it is possible to remove the hatched parts of the domains  $[\mathbf{x}_1]$  and  $[\mathbf{x}_2]$ . **Right Figure:** With  $(\mathbf{x}_1 \bar{\vee} \mathbf{x}_2)_{\epsilon_j^s}$ , it is possible to contract the hatched parts.

Considering a segment  $\epsilon_j^s$  as an obstacle, the visible and non-visible spaces of a box  $[\mathbf{x}]$  regards to the obstacle are delimited by lines. Those lines are passing through the segment bounds and the box vertices (Figure 5). The objective is to identify the extremal lines that characterize the visible and non-visible spaces. It can be noticed that those lines correspond to the lines with the maximal and minimal slopes (Figure 5).

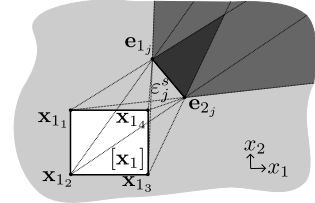


Fig. 5.  $E_{\epsilon_j^s}([\mathbf{x}_1])$  (light grey),  $\tilde{E}_{\epsilon_j^s}([\mathbf{x}_1])$  (medium grey) and  $\bar{E}_{\epsilon_j^s}([\mathbf{x}_1])$  (dark grey) are delimited by lines defined by the segment and box vertices.

*Remark 2:* In order to avoid line singularities, the determinant is used to characterize the lines. Let  $\mathbf{a} = (a_1, a_2)$ ,  $\mathbf{b} = (b_1, b_2)$  and  $\mathbf{c} = (c_1, c_2)$  be three points, the sign of  $\det(\mathbf{a} - \mathbf{b} | \mathbf{c} - \mathbf{b}) = (a_1 - b_1)(c_2 - b_2) - (a_2 - b_2)(c_1 - b_1)$  indicates the *side* of  $\mathbf{a}$  regards to the vector  $\overrightarrow{\mathbf{bc}}$  (Figure 6).

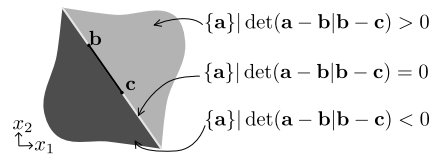


Fig. 6. The sign of  $\det(\mathbf{a} - \mathbf{b} | \mathbf{c} - \mathbf{b})$  depends of the side of  $\mathbf{a}$  regards to  $\overrightarrow{\mathbf{bc}}$ .

1) *Equation of the non-visible space of a box:* The non-visible space of a box  $[\mathbf{x}]$  regards to an obstacle  $\epsilon_j^s = \text{Seg}(\mathbf{e}_{1j}, \mathbf{e}_{2j})$  corresponds to the intersection of the non-visible spaces of the vertices of the box:

$$\bar{E}_{\epsilon_j^s}([\mathbf{x}]) = \bigcap_{z=1}^4 \bar{E}_{\epsilon_j^s}(\mathbf{x}_z), \quad (21)$$

with  $\mathbf{x}_1, \mathbf{x}_2, \mathbf{x}_3, \mathbf{x}_4$  the vertices of the box  $[\mathbf{x}]$  (Figure 5).

*Remark 3:* The following equations correspond to the non-visible space of a point  $\mathbf{x}_z$  regards to an obstacle  $\epsilon_j^s =$

$Seg(\mathbf{e}_{1_j}, \mathbf{e}_{2_j})$

$$\bar{E}_{\mathcal{E}_j^s}(\mathbf{x}_z) = \{ \mathbf{x}_i \mid \begin{array}{l} \zeta_{x_z} \det(\mathbf{x}_i - \mathbf{e}_{1_j} | \mathbf{e}_{2_j} - \mathbf{e}_{1_j}) \leq 0 \quad \wedge \\ \zeta_{x_z} \det(\mathbf{x}_i - \mathbf{x}_z | \mathbf{e}_{1_j} - \mathbf{x}_z) \geq 0 \quad \wedge \\ \zeta_{x_z} \det(\mathbf{x}_i - \mathbf{x}_z | \mathbf{e}_{2_j} - \mathbf{x}_z) \leq 0 \end{array} \}, \quad (22)$$

with

$$\zeta_{x_z} = \begin{cases} 1 & \text{if } \det(\mathbf{x}_z - \mathbf{e}_{1_j} | \mathbf{e}_{2_j} - \mathbf{e}_{1_j}) > 0, \\ -1 & \text{else.} \end{cases}$$

The Figure 7 presents an example of non-visibility characterization. In this example  $\zeta_{x_z} = -1$  (Figure 6).  $\bar{E}_{\mathcal{E}_j^s}(\mathbf{x}_z)$  is then characterized by the points  $\mathbf{x}_i$  such that  $\det(\mathbf{x}_i - \mathbf{e}_{1_j} | \mathbf{e}_{2_j} - \mathbf{e}_{1_j}) \geq 0$  and  $\det(\mathbf{x}_i - \mathbf{x}_z | \mathbf{e}_{1_j} - \mathbf{x}_z) \leq 0$  and  $\det(\mathbf{x}_i - \mathbf{x}_z | \mathbf{e}_{2_j} - \mathbf{x}_z) \geq 0$  (Equation 22). This corresponds to all the points above the line  $(\mathbf{e}_{1_j}, \mathbf{e}_{2_j})$ , under the line  $(\mathbf{x}_z, \mathbf{e}_{1_j})$  and above the line  $(\mathbf{x}_z, \mathbf{e}_{2_j})$  (Figure 6).

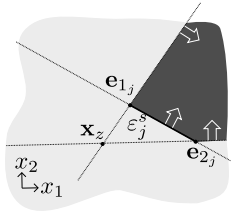


Fig. 7. Example of the non-visible space characterizations.  $\bar{E}_{\mathcal{E}_j^s}(\mathbf{x}_z)$  corresponds to all the points that are under the line  $(\mathbf{x}_z, \mathbf{e}_{1_j})$  and above the line  $(\mathbf{x}_z, \mathbf{e}_{2_j})$  and above the line  $(\mathbf{e}_{1_j}, \mathbf{e}_{2_j})$ .

From the Equations 19 and 21 it can be deduced that

$$(\mathbf{x}_1 \mathbf{V} \mathbf{x}_2)_{\mathcal{E}_j} \Rightarrow [\mathbf{x}_1]^* = [\mathbf{x}_1] \cap \left( \bigcup_{z=1}^4 \bar{E}_{\mathcal{E}_j^s}(\mathbf{x}_z) \right). \quad (23)$$

with  $\mathbf{x}_1 \in [\mathbf{x}_1]$  and  $\mathbf{x}_2 \in [\mathbf{x}_2]$ .

According to the equations 23 and 22 it is possible to build the visibility contractor  $C_V([\mathbf{x}_1], [\mathbf{x}_2], \mathcal{E}_j^s)$ , presented in the Algorithm 1. This contractor uses the backward/forward propagation presented in the Section II-A. It can be noticed that the equations lines 4 to 6 correspond to the complement of the Equation 22 (the  $\wedge$  become  $\vee$  and the signs change).

---

**Algorithm 1:**  $C_V([\mathbf{x}_1], [\mathbf{x}_2], \mathcal{E}_j^s)$

---

**Data:**  $[\mathbf{x}_1], [\mathbf{x}_2], \mathcal{E}_j^s = Seg(\mathbf{e}_{1_j}, \mathbf{e}_{2_j})$

- 1  $\setminus\setminus$  contraction of  $[\mathbf{x}_1]$  ;
  - 2 **for**  $z=1$  **to** 4 **do**
  - 3     backward/forward propagation over
  - 4      $\zeta_{x_z} \det([\mathbf{x}_1] - \mathbf{e}_{1_j} | \mathbf{e}_{2_j} - \mathbf{e}_{1_j}) > 0 \vee$
  - 5      $\zeta_{x_z} \det([\mathbf{x}_1] - \mathbf{x}_z | \mathbf{e}_{1_j} - \mathbf{x}_z) < 0 \vee$
  - 6      $\zeta_{x_z} \det([\mathbf{x}_1] - \mathbf{x}_z | \mathbf{e}_{2_j} - \mathbf{x}_z) > 0$ ;
  - 7      $\setminus\setminus$  The resulting box is noted  $[\mathbf{x}_1]_z^*$ .
  - 8  $[\mathbf{x}_1]^* = \bigcup_{z=1}^4 [\mathbf{x}_1]_z^*$ ;
  - 9  $\setminus\setminus$  The same idea for the contraction of  $[\mathbf{x}_2]$  ;
- Result:**  $[\mathbf{x}_1]^*, [\mathbf{x}_2]^*$ .
- 

2) *Equation of the visible space of a box:* Whereas the computation of the non-visible space of a box can be simplified to the computation of the non-visible spaces of its vertices (Equation 21), for the visible space it is needed to test all the possible lines. Let  $[\mathbf{x}]$  be a box with  $\mathbf{x}_z, z=1, \dots, 4$  its vertices and  $\mathcal{E}_j^s$  an obstacle, the visible space of the box regards to the obstacle can be defined as

$$E_{\mathcal{E}_j^s}([\mathbf{x}]) = \bigcap_{z=1}^4 \{ \mathbf{x}_i \mid \begin{array}{l} (\zeta_{x_z} \det(\mathbf{x}_i - \mathbf{e}_{1_j} | \mathbf{x}_z - \mathbf{e}_{1_j}) > 0 \quad \wedge \\ \zeta_{x_{z+1}} \det(\mathbf{x}_i - \mathbf{e}_{1_j} | \mathbf{x}_{z+1} - \mathbf{e}_{1_j}) > 0 \quad \vee \\ \zeta_{x_z} \det(\mathbf{x}_i - \mathbf{e}_{2_j} | \mathbf{x}_z - \mathbf{e}_{2_j}) < 0 \quad \wedge \\ \zeta_{x_{z+1}} \det(\mathbf{x}_i - \mathbf{e}_{2_j} | \mathbf{x}_{z+1} - \mathbf{e}_{2_j}) < 0 \quad \vee \\ \zeta_{x_z} \det(\mathbf{x}_i - \mathbf{e}_{1_j} | \mathbf{e}_{2_j} - \mathbf{e}_{1_j}) > 0 \quad \wedge \\ \zeta_{x_{z+1}} \det(\mathbf{x}_i - \mathbf{e}_{1_j} | \mathbf{e}_{2_j} - \mathbf{e}_{1_j}) > 0 \quad \wedge \\ (\zeta_{e_1} \det(\mathbf{x}_i - \mathbf{e}_{1_j} | \mathbf{x}_z - \mathbf{e}_{1_j}) > 0 \quad \vee \\ \zeta_{e_1} \det(\mathbf{x}_i - \mathbf{e}_{1_j} | \mathbf{x}_{z+1} - \mathbf{e}_{1_j}) < 0 \quad \wedge \\ (\zeta_{e_2} \det(\mathbf{x}_i - \mathbf{e}_{2_j} | \mathbf{x}_z - \mathbf{e}_{2_j}) > 0 \quad \vee \\ \zeta_{e_2} \det(\mathbf{x}_i - \mathbf{e}_{2_j} | \mathbf{x}_{z+1} - \mathbf{e}_{2_j}) < 0 \quad \vee \end{array} \}. \quad (24)$$

with

$$\mathbf{x}_5 = \mathbf{x}_1,$$

$$\zeta_{x_z} = \begin{cases} 1 & \text{if } \det(\mathbf{x}_z - \mathbf{e}_{1_j} | \mathbf{e}_{2_j} - \mathbf{e}_{1_j}) > 0, \\ -1 & \text{else.} \end{cases}$$

$$\zeta_{x_{z+1}} = \begin{cases} 1 & \text{if } \det(\mathbf{x}_{z+1} - \mathbf{e}_{1_j} | \mathbf{e}_{2_j} - \mathbf{e}_{1_j}) > 0, \\ -1 & \text{else.} \end{cases}$$

$$\zeta_{e_2} = \begin{cases} 1 & \text{if } \det(\mathbf{e}_{1_j} - \mathbf{x}_z | \mathbf{x}_{z+1} - \mathbf{x}_z) > 0, \\ -1 & \text{else.} \end{cases}$$

$$\zeta_{e_2} = \begin{cases} 1 & \text{if } \det(\mathbf{e}_{2_j} - \mathbf{x}_z | \mathbf{x}_{z+1} - \mathbf{x}_z) > 0, \\ -1 & \text{else.} \end{cases}$$

The first six relations of the Equation 24 determinate the lines with the maximal and minimal slopes. The last four equations deal with a singularity presented in the Figure 8. Without those four equations, the partial-visible space (medium grey) could be considered as included in the visible space.

Note that the non-visibility contractor  $C_{\bar{V}}([\mathbf{x}_1], [\mathbf{x}_2], \mathcal{E}_j^s)$  can be built as it is done for the visibility contractor presented in the Section IV-1.

## V. THE POSE TRACKING ACCORDING TO THE VISIBILITY

### A. The Pose Tracking Algorithm

As mentioned in the introduction we are interested in the pose tracking localization problem. Knowing the initial pose  $\mathbf{q}_i(k_0)$  of a robot  $r_i$ , the objective is to estimate the pose  $\mathbf{q}_i(k)$  at each time  $k$ . Using the dynamic equation of the system (Section I) it is possible to compute the pose of the robots at time  $k$  knowing the pose at time  $k-1$ . To be able to

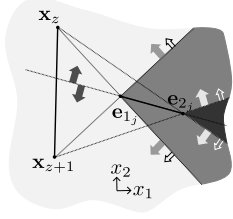


Fig. 8. Example of the visible space characterizations (light grey space). The arrows correspond to the several constraints of the Equation 24 (ten relations, ten arrows). The filled arrows correspond to the first six constraints, and the empty ones to the last four constraints. As in the other figures, the light grey area corresponds to the visible space, the medium grey to the partial-visible space and the dark grey to the non-visible space.



Fig. 9. The three simulated environments  $\mathcal{E}_1$ ,  $\mathcal{E}_2$  and  $\mathcal{E}_3$ . The black shapes correspond to the obstacles and the grey dotted lines delimited the space of the robots moves.

compute the new pose, the orientation  $\theta_i(k)$  is measured by the compass and the input vector  $\mathbf{u}_i(k)$  is estimated by the odometry. In order to deal with the sensor imprecisions, we consider a bounded error context. Thus it is possible to define  $[\theta_i(k)]$  and  $[\mathbf{u}_i(k)]$  according to the sensors' measurements, such that  $\theta_i(k) \in [\theta_i(k)]$  and  $\mathbf{u}_i(k) \in [\mathbf{u}_i(k)]$ , and  $[\mathbf{q}_i(k_0)]$  the initial robot's pose estimation such that  $\mathbf{q}_i(k_0) \in [\mathbf{q}_i(k_0)]$ . In this context it is possible to compute the pose  $[\mathbf{q}_i(k+1)] = f([\mathbf{q}_i(k)], [\mathbf{u}_i(k)])$  using interval analysis principles.

In order to avoid the drifting of the robots (the increase of  $[\mathbf{q}_i(k)]$  size), the visibility information between the robots is considered. At each time  $k$  each robot computes the visibility information regards to the other robots of the team. Let  $r_i$  and  $r_{i'}$  be two different robots of  $\mathcal{R}$ ,

$$r_i \text{ sees } r_{i'} \Leftrightarrow (\mathbf{x}_i \nabla \mathbf{x}_{i'})_{\mathcal{E}}, \quad (25)$$

$$r_i \text{ does not see } r_{i'} \Leftrightarrow (\mathbf{x}_i \bar{\nabla} \mathbf{x}_{i'})_{\mathcal{E}}. \quad (26)$$

It is also needed that at each time  $k$ , each robot  $r_i$  communicates its current pose estimation  $[\mathbf{q}_i(k)]$  with the team  $\mathcal{R}$ .

Algorithm 2 presents the proposed pose tracking approach. First, Line 1, the initial poses of the robots are defined. Line 3, for each robots, the new pose is estimated regards to the knowledge of the previous one. Line 4, the robots share their pose estimations with the team. Finally, Lines 5 to 9 the visibility information is used to contract the robot's pose estimations. Lines 7 and 9, two contractors are used: the visibility contractor  $C_{\nabla}$  and the non-visibility contractor  $C_{\bar{\nabla}}$ . The objective of those functions is to remove from the domains  $[\mathbf{x}_i]$  and  $[\mathbf{x}_{i'}]$ , the values that are not consistent with the visibility and non-visibility informations. They are detailed in the previous Section.

---

### Algorithm 2: The pose tracking algorithm

---

**Data:**  $\mathcal{R}$ ,  $\mathcal{E}^-$ ,  $\mathcal{E}^+$

```

1  $\forall r_i \in \mathcal{R}$ , initialize  $[\mathbf{q}_i(k_0)]$ ;
2 for  $k = 1$  to end do
3    $\forall r_i \in \mathcal{R}$ ,  $[\mathbf{q}_i(k)] = f([\mathbf{q}_i(k-1)], [\mathbf{u}_i(k-1)])$ ;
4    $\forall r_i \in \mathcal{R}$ , share  $[\mathbf{q}_i(k)]$  with the team;
5   forall the  $r_i \in \mathcal{R}$ ,  $r_{i'} \in \mathcal{R}$ ,  $r_i \neq r_{i'}$  do
6     if  $r_i$  sees  $r_{i'}$  then
7        $([\mathbf{x}_i(k)]^*, [\mathbf{x}_{i'}(k)]^*) =$ 
8          $\bigcap_{\forall \mathcal{E}_j^- \in \mathcal{E}^-} \{C_{\nabla}([\mathbf{x}_i(k)], [\mathbf{x}_{i'}(k)], \mathcal{E}_j^-\)}\}$ ;
9     else
10       $([\mathbf{x}_i(k)]^*, [\mathbf{x}_{i'}(k)]^*) =$ 
11         $\bigcup_{\forall \mathcal{E}_j^+ \in \mathcal{E}^+} \{C_{\bar{\nabla}}([\mathbf{x}_i(k)], [\mathbf{x}_{i'}(k)], \mathcal{E}_j^+)\}$ ;

```

---

### B. Experimental Results

In order to test this approach, a simulator has been developed. The efficiency of the algorithm has been tested for three different environments  $\mathcal{E}_1$ ,  $\mathcal{E}_2$  and  $\mathcal{E}_3$  (Figure 9). Each environment has a  $10 \times 10$  m<sup>2</sup> size. It can be noticed that the simulated environments are polygonal. This has been done in order to simplify the computation of simulated data. The proposed algorithm manipulates only the inner and outer characterisations and would work as well in a non-polygonal environments (the characterisations considered for the presented experimentations are not perfect and could have been associated to non-polygonal shapes).

The following table presents the number of segments of the characterisations of each environment:

	$\mathcal{E}_1$	$\mathcal{E}_2$	$\mathcal{E}_3$
$\mathcal{E}^-$	19	59	89
$\mathcal{E}^+$	26	69	101

At each iteration (one moving and one contraction step) a robot does a 20cm distance move, with a bounded error of  $\pm 1\%$ , and has a bounded compass error of  $\pm 1$  deg. Note that  $\forall r_i \in \mathcal{R}$ ,  $[\mathbf{x}_i(k_0)] = [\mathbf{x}_i(k_0) - 50\text{cm}, \mathbf{x}_i(k_0) + 50\text{cm}]$ .

The processor used for the simulations has the following characteristics: Intel(R) Core(TM) CPU - 6420 @ 2.13GHz.

During those tests the simulated robots moved randomly in the environment, from  $k_0 = 0$  to  $k = 1500$ . The results of the experimentations are presented in the Table I. Note that *average*  $w([x_{\{1,2\}_i}])$  corresponds to the average size of  $[x_{\{1,2\}_i}]$  during the all experimentation and *final*  $w([x_{\{1,2\}_i}])$  corresponds to the average of  $[x_{\{1,2\}_i}]$  just for the final step.

As it can be noticed that the size of the initial boxes  $w([x_{\{1,2\}_i}])$  are equal to 100cm (initial incertitude about the position). It can be concluded that the experimentations providing a final incertitude around 100cm (or smaller) lead to successful localizations (avoiding the drifting of the robots). In addition to that it is possible to classify as successful the experimentations that have: *average*  $w([x_{\{1,2\}_i}]) \approx$  *final*  $w([x_{\{1,2\}_i}])$  (the imprecision is maintained and do not increase).

		number of robots					
		4	8	12	16	20	24
$\mathcal{E}_1$	average $w(x_{1i})$	439	310	<b>196</b>	<b>131</b>	<b>127</b>	<b>115</b>
	average $w(x_{2i})$	460	334	<b>176</b>	<b>147</b>	<b>121</b>	<b>117</b>
	final $w(x_{1i})$	897	668	<b>172</b>	<b>147</b>	<b>121</b>	<b>117</b>
	final $w(x_{2i})$	919	674	<b>193</b>	<b>167</b>	<b>159</b>	<b>133</b>
	iteration time	3	28	92	204	351	589
$\mathcal{E}_2$	average $w(x_{1i})$	545	355	183	<b>102</b>	<b>93</b>	<b>84</b>
	average $w(x_{2i})$	552	375	185	<b>115</b>	<b>108</b>	<b>97</b>
	final $w(x_{1i})$	1029	780	440	<b>107</b>	<b>100</b>	<b>62</b>
	final $w(x_{2i})$	1038	811	435	<b>110</b>	<b>97</b>	<b>95</b>
	iteration time	11	65	191	443	745	1160
$\mathcal{E}_3$	average $w(x_{1i})$	404	<b>120</b>	<b>75</b>	<b>62</b>	<b>63</b>	<b>56</b>
	average $w(x_{2i})$	325	<b>77</b>	<b>59</b>	<b>50</b>	<b>47</b>	<b>46</b>
	final $w(x_{1i})$	817	<b>126</b>	<b>81</b>	<b>69</b>	<b>87</b>	<b>47</b>
	final $w(x_{2i})$	688	<b>65</b>	<b>58</b>	<b>50</b>	<b>57</b>	<b>45</b>
	iteration time	15	116	313	646	1058	1727

Without the visibility information - odometry and compass only -			
average $w(x_{1i})$	588	final $w(x_{1i})$	1075
average $w(x_{2i})$	595	final $w(x_{2i})$	1084

TABLE I

EXPERIMENTAL RESULTS (the values are in cm and ms).

Those successful experimentations are depicted in bold in Table I. *Iteration time* correspond to the average iteration time of the 1500 iteration step time (in ms).

Looking at those results it appears that two elements are important factors for the success of the localization: the topology of the environment and the number of robots.

It appears that for a given environment a minimal number of robots is necessary to perform an efficient pose tracking. It can be explained by the fact that with few robots, the visibility measurements carry few informations. In our experimentations, at least 8 robots are necessary to perform an efficient localization in the environment  $\mathcal{E}_3$ , 12 for the environment  $\mathcal{E}_1$  and 16 for the environment  $\mathcal{E}_2$ . On the other hand, too many robots does not improve significantly the localization but increase the computation time.

It also appears that for a given number of robots the localization process can be efficient in one environment whereas it is not in the others. For instance with a team of 8 robots, the algorithm provides a good localization in the environment  $\mathcal{E}_3$ , but not in the environment  $\mathcal{E}_1$  neither in  $\mathcal{E}_2$ . The number of obstacles, their sizes and their dispositions in the environment are important factors for an efficient localization. It can be explained by the fact that without any obstacle, or with too small obstacles, the robots see each other constantly, thus the visibility sensor will return always the same value and will not provide useful information. It is the same argument with too many obstacles.

### C. Conclusion

In this paper it is shown that using interval analysis it is possible to localize a team of robots only assuming weak informations: the visibility between the robots. The proposed algorithm is a guaranteed method that is able to exploit this boolean information. Note that the context of the presented experimentations is borderline as it only considers the weak

boolean visibility information. In practice this information can be added to classical localization methods, using range sensors for example, when a team of robots is considered, as in [15], [16].

It appears in Section V-B that the topology of an environment is an important factor for the efficiency of the proposed localization. In a future work it could be interesting to characterize the environments, allowing to calculate for a given environment, a minimal number of robots required to perform a pose tracking.

Finally we are planning to consider a maximal range for the visibility information and to restrain the field of vision of the robots.

### REFERENCES

- [1] J. Borenstein, H. R. Everett, and L. Feng, *Navigating Mobile Robots: Systems and Techniques*. A. K. Peters, Ltd., 1996.
- [2] M. Segura, V. Mut, and H. Patino, "Mobile robot self-localization system using ir-uwv sensor in indoor environments," in *Robotic and Sensors Environments, 2009. ROSE 2009. IEEE International Workshop on*, nov. 2009, pp. 29–34.
- [3] J. Zhou and L. Huang, "Experimental study on sensor fusion to improve real time indoor localization of a mobile robot," in *Robotics, Automation and Mechatronics (RAM), 2011 IEEE Conference on*, sept. 2011, pp. 258–263.
- [4] P. Jensfelt and H. Christensen, "Pose tracking using laser scanning and minimalistic environmental models," *Robotics and Automation, IEEE Transactions on*, vol. 17, no. 2, pp. 138–147, apr 2001.
- [5] K. Lingemann, A. Nehter, J. Hertzberg, and H. Surmann, "High-speed laser localization for mobile robots," *Robotics and Autonomous Systems*, vol. 51, no. 4, pp. 275–296, 2005.
- [6] P. Abeles, "Robust local localization for indoor environments with uneven floors and inaccurate maps," in *Intelligent Robots and Systems (IROS), 2011 IEEE/RSJ International Conference on*, sept. 2011, pp. 475–481.
- [7] I. Rekleitis, G. Dudek, and E. Milios, "Multi-robot collaboration for robust exploration," in *Robotics and Automation, 2000. Proceedings. ICRA '00. IEEE International Conference on*, vol. 4, 2000, pp. 3164–3169.
- [8] F. Dellaert, F. Alegre, and E. B. Martinson, "Intrinsic localization and mapping with 2 applications: Diffusion mapping and marco polo localization," in *Proceedings of the IEEE International Conference on Robotics and Automation*, 2003, pp. 2344–2349.
- [9] P. Giguere, I. Rekleitis, and M. Latulippe, "I see you, you see me: Cooperative localization through bearing-only mutually observing robots," in *Intelligent Robots and Systems (IROS), 2012 IEEE/RSJ International Conference on*, 2012, pp. 863–869.
- [10] E. Seignez, M. Kieffer, A. Lambert, E. Walter, and T. Maurin, "Experimental vehicle localization by bounded-error state estimation using interval analysis," in *Intelligent Robots and Systems, 2005. (IROS 2005). 2005 IEEE/RSJ International Conference on*, aug. 2005, pp. 1084–1089.
- [11] L. Jaulin, "A nonlinear set membership approach for the localization and map building of underwater robots," *Robotics, IEEE Transactions on*, vol. 25, no. 1, pp. 88–98, feb. 2009.
- [12] L. Jaulin, M. Kieffer, O. Didrit, and E. Walter, *Applied Interval Analysis*. Springer, 2001.
- [13] A. Neumaier, *Interval Methods for Systems of Equations (Encyclopedia of Mathematics and its Applications)*. Cambridge University Press, 1991.
- [14] F. Rossi, P. Beek, and T. Walsh, *Handbook of Constraint Programming (Foundations of Artificial Intelligence)*. Elsevier Science Inc., 2006.
- [15] D. Fox, W. Burgard, H. Kruppa, and S. Thrun, "A probabilistic approach to collaborative multi-robot localization," *Auton. Robots*, vol. 8, no. 3, pp. 325–344, jun 2000.
- [16] I. Rekleitis, G. Dudek, and E. Milios, "Multi-robot cooperative localization: a study of trade-offs between efficiency and accuracy," in *Intelligent Robots and Systems, 2002. IEEE/RSJ International Conference on*, vol. 3, 2002, pp. 2690–2695 vol.3.